

Article

Annual Trends of Soil Moisture and Rainfall Flux in an Arid Climate Using Remote Sensing Data

Mohammad Valipour^{1,2,*}, Helaleh Khoshkam², Sayed M. Bateni³ and Essam Heggy^{3,4}

¹ Department of Engineering and Engineering Technology, Metropolitan State University of Denver, Denver, CO 80217, USA; E-Mail: mvalipou@msudenver.edu

² Department of Civil and Environmental Engineering and Water Resources Research Center, University of Hawaii at Manoa, Honolulu, HI 96822, USA; E-Mails: helaleh@hawaii.edu; smbateni@hawaii.edu

³ Viterbi School of Engineering, University of Southern California, Los Angeles, CA 90089, USA; E-Mail: heggy@usc.edu

⁴ Jet Propulsion Laboratory, California Institute of Technology, Pasadena, CA 91109, USA

* For correspondence.

Abstract The water crisis is still a major issue in Qatar. Seawater desalination has been strongly implemented in the Persian Gulf region. However, it is costly and there is corrosion in piping materials and other equipment. Hence, there is a vital need to detect groundwater resources in Qatar. Various factors affect the variability of groundwater in Qatar including hydrogeological aspects, climate change, drawdown and abstraction, rainwater harvesting, desertification, and population growth. In this study, we employ the Famine Early Warning Systems Network (FEWS NET) Land Data Assimilation System (FLDAS) to monitor annual variations of soil moisture (SM) in the depth of 1–2 m (as an indicator of groundwater) and rainfall flux (RF) from 1982 to 2019. The results show that SM and RF anomalies were positive from 1982 to 2000 (except 1992). In contrast, these anomalies became negative during 2001–2019 (except 2001 and 2018), implying the drawdown of groundwater resources. Drier years (i.e., negative RF anomaly) in the recent 19 years (2001–2019) reduced SM and led to a negative SM anomaly. The Mukaynis and Wadi Jallal regions (located in Al Rayyan and Al Wakrah municipalities, respectively) had the highest RF and SM from 1982 to 2019. The center-pivot irrigation systems close to the Mukaynis and Wadi Jallal regions indicate their accessibility to groundwater resources in Qatar. Moreover, these regions have the lowest risk of salinization and groundwater vulnerability. In addition, annual trends of groundwater storage (GWS) retrieved from the Gravity Recovery and Climate Experiment (GRACE) from 2003 to 2019 have been presented. This study is beneficial for detecting and monitoring groundwater resources for the sustainable management of water resources in arid environments.

Keywords Qatar; groundwater; soil moisture; rainfall; arid regions; sustainable systems engineering; GRACE, annual anomaly; FLDAS

Open Access

Received: 1 July 2022

Accepted: 17 August 2022

Published: 18 August 2022

Academic Editor

Hossein Bonakdari, University of Ottawa, Canada

Copyright: © 2022 Valipour et al. This article is distributed under the terms of the [Creative Commons Attribution License](#) (CC BY 4.0), which permits unrestricted use and distribution provided that the original work is properly cited.

1. Introduction

1.1. Literature Review

Qatar is an arid country with limited water resources. It has low rainfall with an annual mean of about 75 mm. The fossil groundwater reserves, which are predominantly stored in the sedimentary formations of the Arabian platform constitute the main water resources in Qatar [1,2]. The total groundwater abstraction in Qatar is 2.5×10^8 m³ per year. On the other hand, the population is growing rapidly with the high rate of migrant workers from other Arab countries, Pakistan, India, and Europe, increasing the water demand [3]. The population of Qatar has exponentially increased from about 5.0×10^4 in 1960 to almost 2.5×10^6 in 2015. As a result, the limited natural renewable water resources in Qatar have been overexploited. The country's water consumption per capita is 500 lit/day, which is the highest in the world [4]. Aquifers are the only source of natural water in Qatar [4]. Extensive groundwater pumping for irrigation during the last few decades has resulted in a substantial decline in groundwater levels and deterioration of groundwater quality [4]. At present, no big storage facility for the desalinated water

Highlights of Science

exists, and the stored water is enough for two days of supply. Therefore, one of the main grand challenges in Qatar is to detect new groundwater resources and diversify water resources [4].

The major water storage in the Arabian Peninsula (including Qatar) is located on the Arabian platform within formations of the Tertiary age. The Tertiary aquifer systems on the Arabian platform were investigated by many researchers. For example, Al-Ibrahim [5], Bakiewicz et al. [6], Beaumont [7], and Pike [3] studied the development of water resources in the main giant aquifers in the Arabian Peninsula. Dirks et al. [8] studied the hydrological aspects of the Umm er Radhuma aquifer in the Arabian Peninsula. Al-Fatlawi [9,10] focused on the geological and hydrogeological characteristics of the Umm er Radhuma aquifer in western Iraq. Aquifers in the Arabian Peninsula countries were also investigated by the Food and Agriculture Organization (FAO) [11].

There is a high potential for evaporation in arid climates [12–14]. Evaporation in dry climates forms salt pans as a sign of significant water loss from the groundwater aquifers [15–17]. The use of groundwater resources in arid regions is still a significant issue. The main challenge is the growing discrepancy between the water demand and supply, in particular in the Arabian Peninsula, which is the driest part of the world [18]. Hence, the importance of detecting groundwater resources in the Arabian Peninsula has received much attention on the global level [19–24].

Recently, several efforts were focused on evaluating the sustainability of groundwater sources for different scenarios. Kalhor and Emaminejad [19] studied the influence of groundwater availability on the growth of cities via remote sensing data. Awad [25] evaluated the deterioration of groundwater in Egypt. Lanjwani et al. [20] assessed the risk of heavy metals in groundwater resources on humans. Bedaso et al. [21] assessed groundwater sustainability in the State of Ohio (USA) under climate change using isotopic tracers and climate models. Numerous other studies were conducted to understand the influence of groundwater withdrawal on the environment [22–24,26].

In the Arabian Peninsula, the non-renewable groundwater is mainly sourced from the sedimentary and deep rock aquifers, which serve as a reservoir of the “fossil” water formed over 1000 to 32,000 years ago [27]. Palaeohydrological evidence has suggested that groundwater recharge occurs sometimes during the Late Pleistocene glaciation or the Early Holocene period. However, failing to recharge the total groundwater storage nowadays made the fossil aquifers “storage-dominated” rather than “recharge-flux-dominated” [28]. The decline of the groundwater levels can be attributed to extracting more water than can be naturally replaced by recharge. Milewski et al. [29] developed a groundwater risk index to evaluate groundwater depletion in the Middle East and North Africa (MENA) region. They showed that Qatar has the second-highest groundwater risk index among all countries in the region.

Qatar suffers mainly from water scarcity, which will be more severe due to global warming [4]. Qatar does not have surface freshwater resources [4,30]. The water demand in Qatar will be 2.5×10^9 m³ in 2025 and about 60% of that will be used in the agricultural sector. Hence, water consumption is anticipated to be much higher than rainfall [1]. Also, the water table in the urban areas of Qatar has shown drawdown due to rapid urbanization [1,31].

Ministry of Development Planning and Statistics (MDPS) [32] reported that Qatar relies on seawater desalination as the primary source of drinking water and groundwater abstraction as the main source of agriculture. MDPS [33] warned that the fresh groundwater reserves are still being overexploited, which leads to a lower groundwater level and a higher water salinity. Indeed, all groundwater resources in Qatar are overexploited over their safe yield by about five times. This has reduced the quality of groundwater resources [30].

To the best of our knowledge, no study analyzed the long-term annual trends of soil moisture (SM) and rainfall in Qatar using remote sensing data. The objective of this work is to study the annual trends of soil moisture at the depth of 1–2 m and rainfall (RF) in Qatar from 1982 to 2019. It is hypothesized that regions with the highest SM have more accessibility to groundwater resources.

1.2. Geographical and Climatic Characteristics of Qatar

Qatar is a semi-arid country in the east of the Arabian Peninsula, which spans over the 24.27°N–26.10°N and 50.45°E–51.40°E [32]. It has a length of ~180 km, a width of ~90 km, and an area of ~11,586 km² [34]. Qatar has mainly a flat rocky surface and consists of some hills with an elevation of up to 103 m above sea level [32]. The north of Qatar has relatively a low

elevation (6 m above the sea level in Dukhan Sabkha), which increases gradually up to 103 m in the west and southwest [35]. It is mostly located over a uniform limestone bed [32].

Qatar has an arid climate. It is characterized by hot summers that last at least four months, cold winters that continue about three months, and short transitional springs and falls. It suffers from water scarcity and drought. Rainfall is limited to certain months, starting mainly in October and ending in May. The peak of rainfall occurs in winter. The rainfall in winter exceeds 50% of the total annual rainfall [1].

The air temperature and drought are increasing steadily, which lead to the use of groundwater resources at a faster rate that can be compensated by rainfall, and therefore a decline in freshwater availability. The heat will increase the incidence of extreme weather events such as hurricanes. Qatar is one of the most sensitive areas to climate change [36]. The average annual rainfall, air temperature, and relative humidity in Qatar vary over the range of 75–200 mm, 20–35 °C, and 40–60%, respectively [37]. A huge amount of water is lost due to evaporation, which exceeds the rainfall rate. The Intergovernmental Panel on Climate Change (IPCC) estimates an increase of up to 2 °C in air temperature in the next 15–20 years and over 4 °C by the end of the century in Qatar [38].

2. Materials and Methods

Famine Early Warning Systems Network (FEWS NET) Land Data Assimilation System (FLDAS) was developed to produce hydrological fluxes and states with a spatial resolution of 0.1° and temporal sampling of one month over some parts of Africa and the Middle East [39].

Using rainfall, air temperature, relative humidity, solar radiation, and wind speed data from in-situ measurements, land surface models, and satellite remote sensing retrievals, the FLDAS generates multi-model and multi-forcing estimations of hydroclimatological data including rainfall flux, surface and root zone soil moisture, actual evapotranspiration, and runoff [39,40]. The FLDAS was created under the NASA Applied Sciences Program by the joint efforts of the U.S. Geological Survey (USGS) Earth Resources Observation and Science (EROS) Center, NASA Goddard Space Flight Center (GSFC), and the University of California Santa Barbara (UCSB) Climate Hazards Group (CHG). The FLDAS variables are required for water resources management and monitoring and are used to produce indices such as surface and root zone soil moisture percentiles that show how current hydrologic extremes compare to conditions over the past three decades. Within FEWS NET, FLDAS outputs are combined with remotely sensed estimates, ground observations, and reports from fields to identify potential food security crises. FEWS NET reports regarding the 2015 Ethiopia and 2015–2016 Southern Africa droughts are examples of this approach [39,41].

In this study, we analyzed the annual trends of FLDAS SM data (in the depth of 1–2 m) in Qatar from 1982 to 2019 (38 years) as an indicator of groundwater. The soil depth of 1–2 m was also used for groundwater monitoring in the previous investigations [40–46]. Based on a piezometric survey in 2009, Baalousha [34] indicated that the depth of the water table in most regions of Qatar is 1–2 m (Figure 1). In this study, variations of rainfall flux (RF) are also evaluated in the same 38-year period (1982–2019). We also assess the variations of SM and RF anomalies during 1982–2019. Finally, areas/cities in Qatar with the highest SM values are identified.

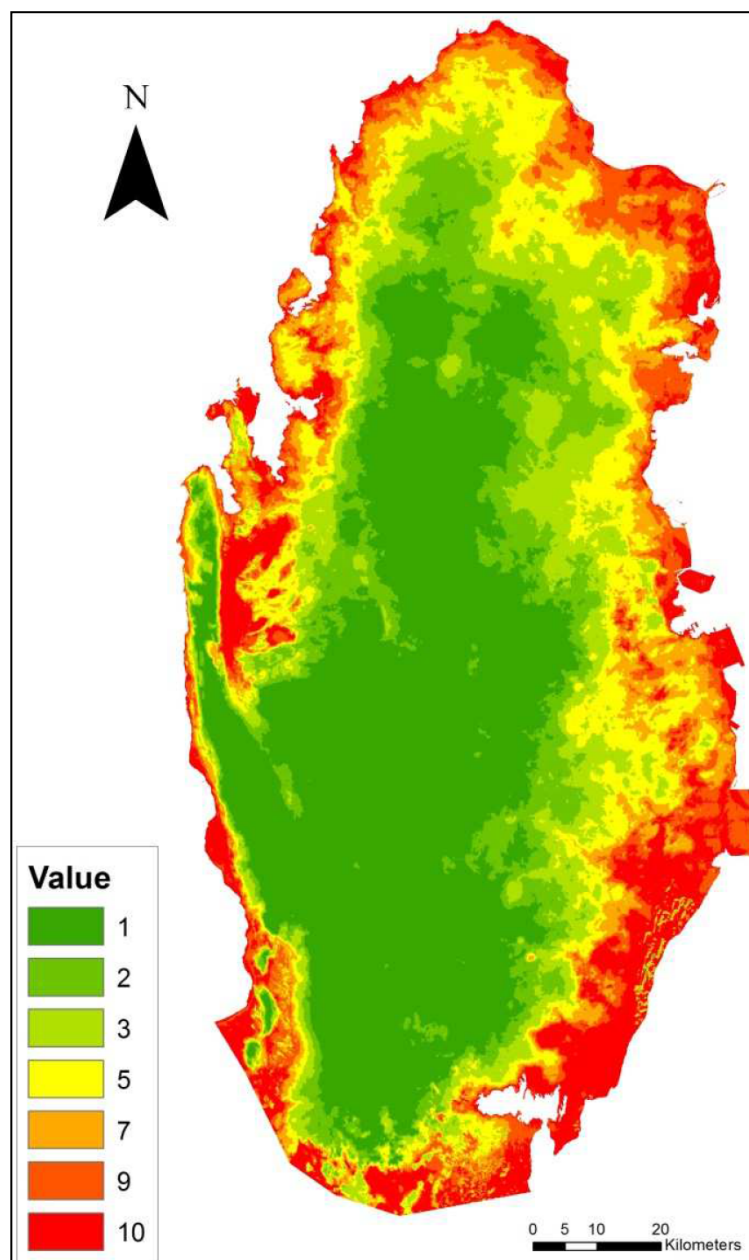


Figure 1. Depth (m) to the water table in Qatar (adapted from [34]).

3. Results and Discussions

Figure 2 shows the annual SM data in Qatar from 1982 to 2019. As can be seen, the highest spatially-averaged SM (\overline{SM}) of $0.35 \text{ (m}^3/\text{m}^3)$ occurred in 1995, 1996, and 1997. Also, the lowest \overline{SM} of $0.32 \text{ (m}^3/\text{m}^3)$ happened in 2012–2016. \overline{SM} increased in recent years (2017–2019) due to the increase in rainfall (see Figures 2 and 4). Figure 3 shows maps of mean SM from 1982–2000 and 2001–2019. In general, SM data over Qatar showed lower values in 2001–2019 than in 1982–2000. It is worth mentioning that the range of variability of \overline{SM} in different years is low (changes from $0.32 \text{ (m}^3/\text{m}^3)$ to $0.35 \text{ (m}^3/\text{m}^3)$) because it represents the SM in the depth of 1–2 m, and not the land surface.

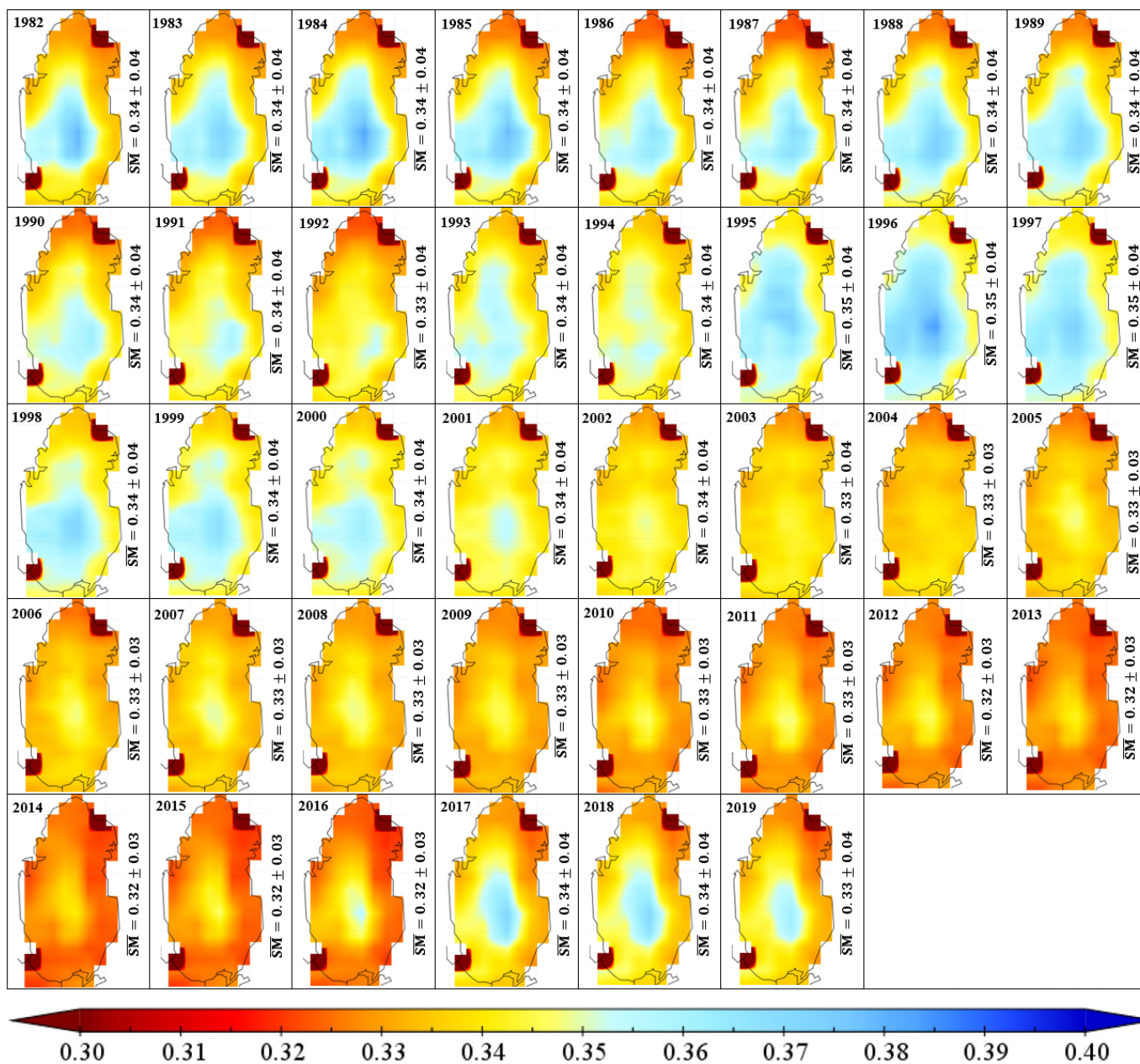


Figure 2. Annual maps of soil moisture (m^3/m^3) in Qatar from 1982 to 2019. Spatially-averaged soil moisture (\overline{SM}) plus/minus one standard deviation is shown on each map.

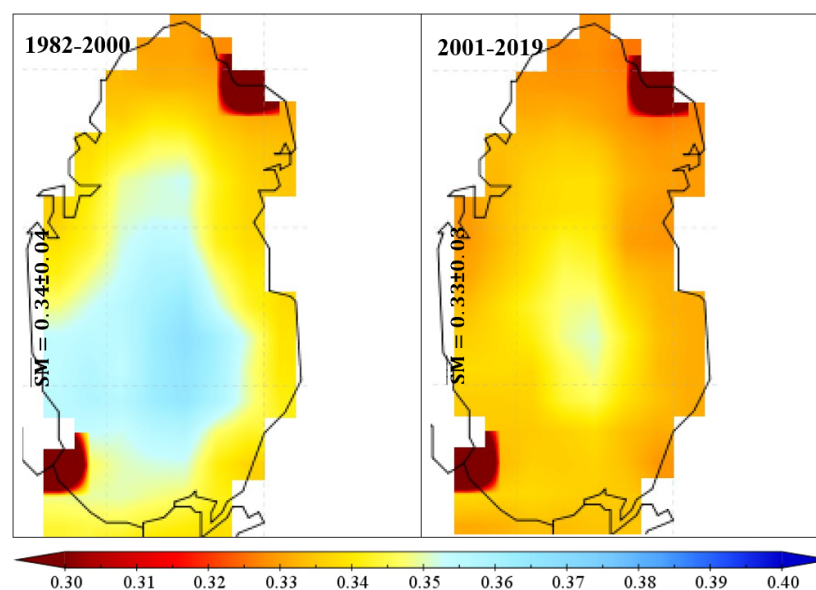


Figure 3. Maps of mean soil moisture (m^3/m^3) during 1982–2000 (left) and 2001–2019 (right). Spatially-averaged soil moisture (SM) plus/minus one standard deviation is also shown on each map.

Rainfall is the only source to recharge groundwater in Qatar [1]. Figure 4 demonstrates the annual maps of RF in Qatar from 1982 to 2019. The highest and lowest RF data are observed in 1982 and 2010, respectively, with the spatially-averaged values of $6.14 \text{ (mg/m}^2/\text{s)}$ and $1.58 \text{ (mg/m}^2/\text{s)}$. The year 2010 is well known as a dry year and several studies reported drought conditions for this year in the Middle East [47,48]. A comparison of Figures 2 and 4 indicates that three major rainfall events before 1983, 1995–1996, and in 2017 recharged groundwater resources and increased SM for the periods 1982–1991, 1995–2000, and 2017–2019, respectively. A consistent spatial variability is seen in the RF maps from 1982 to 2019, i.e., RF is at its peak around the center of Qatar and decreases toward its borders. A similar spatial pattern is observed in the SM maps (Figure 2) in which SM is highest in the central areas of Qatar and decreases to its borders. The spatiotemporal consistency between the RF and SM maps (Figures 2 and 4) implies that SM is mainly controlled by rainfall in Qatar.

Figure 5 shows maps of mean RF during the past (1982–2000) and recent (2001–2019) 19 years. The mean rainfall data in 2001–2019 is lower than that of 1982–2000, which is consistent with the lower mean SM in 1982–2000 compared to 2001–2019.

Figure 6 indicates the annual maps of SM anomaly (δSM) in Qatar from 1982–2019. The highest and lowest SM anomalies are observed in 1996 and 2014, respectively. SM anomalies are positive over most parts of Qatar from 1982–2000 (except in 1992). In contrast, SM anomalies became negative in most regions from 2001–2019 (except in 2001 and 2018). Figure 7 shows maps of mean soil moisture anomaly during 1982–2000 and 2001–2019. According to Figure 7, SM anomalies are positive in the past 19 years (1982–2000), but they are negative during the recent 19 years (2001–2019), which indicates increasing drought and declining groundwater in Qatar. Valipour et al. [49] reported the year 2000 as an inflection point in Iran, which is a neighboring country located in the north of Qatar. As shown in Valipour et al. [49], positive and negative trends of rainfall were observed in Iran before and after 2000, respectively, which affect δSM and are in line with our results in Figures 6 and 7.

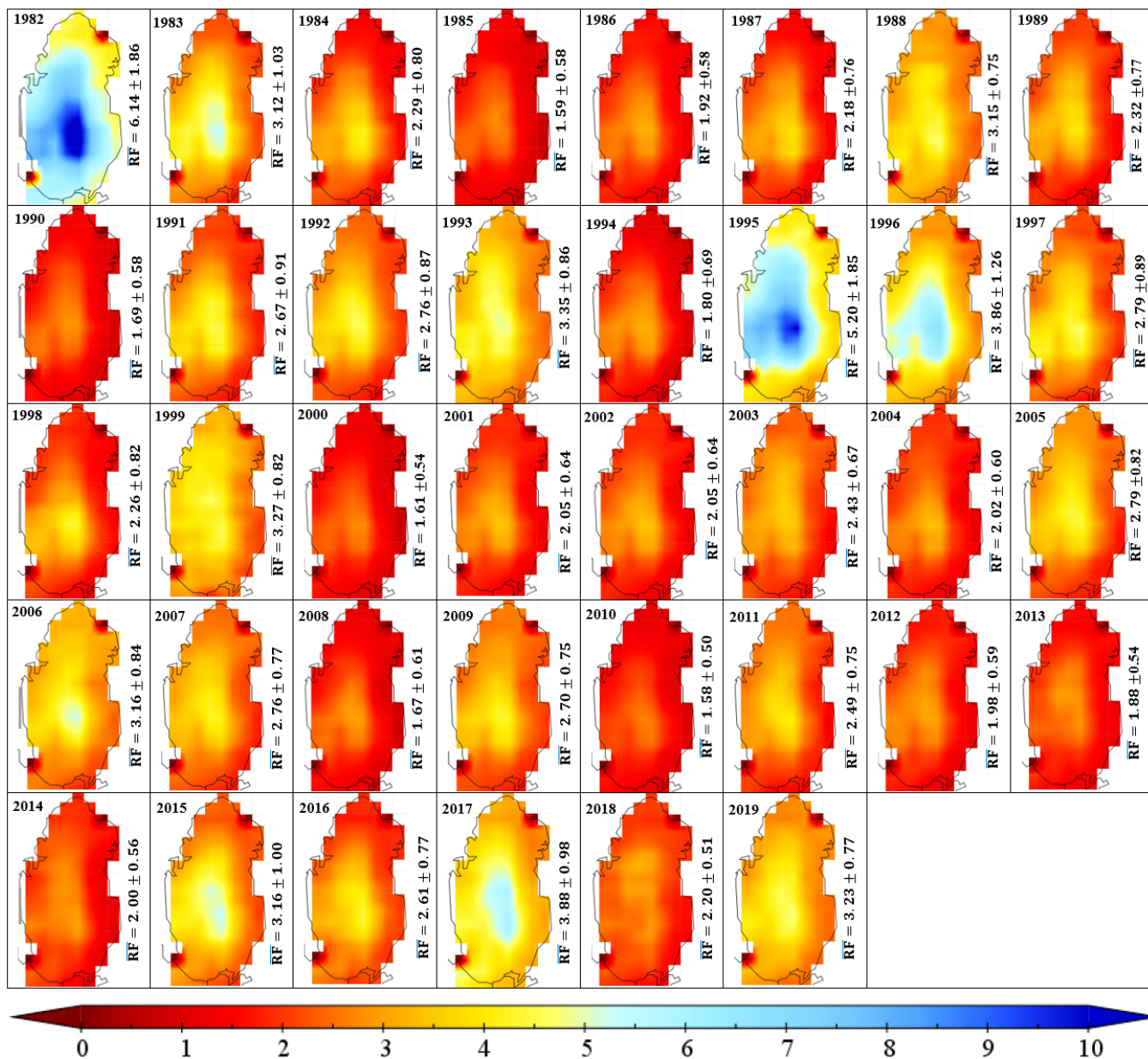


Figure 4. Maps of annual rainfall flux (mg/m²/s) in Qatar from 1982 to 2019. Spatially-averaged rainfall flux (\overline{RF}) plus/minus one standard deviation value is shown on each map.

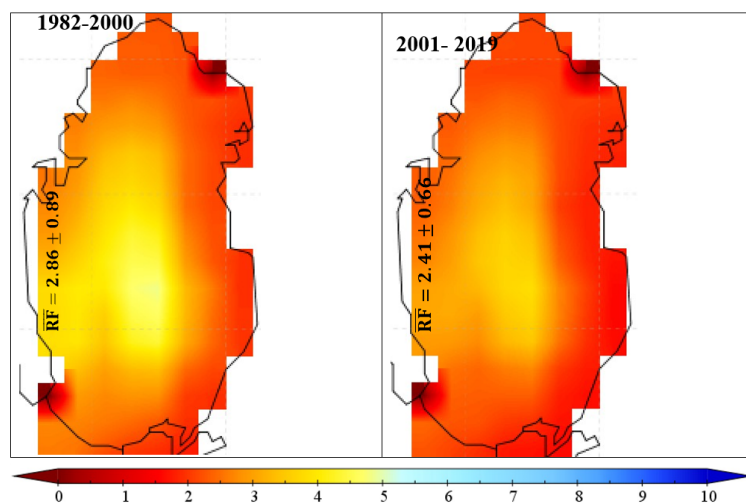


Figure 5. Maps of mean rainfall flux (mg/m²/s) during 1982–2000 (left) and 2001–2019 (right). Spatially-averaged rainfall flux (\overline{RF}) plus/minus one standard deviation is also shown on each map.

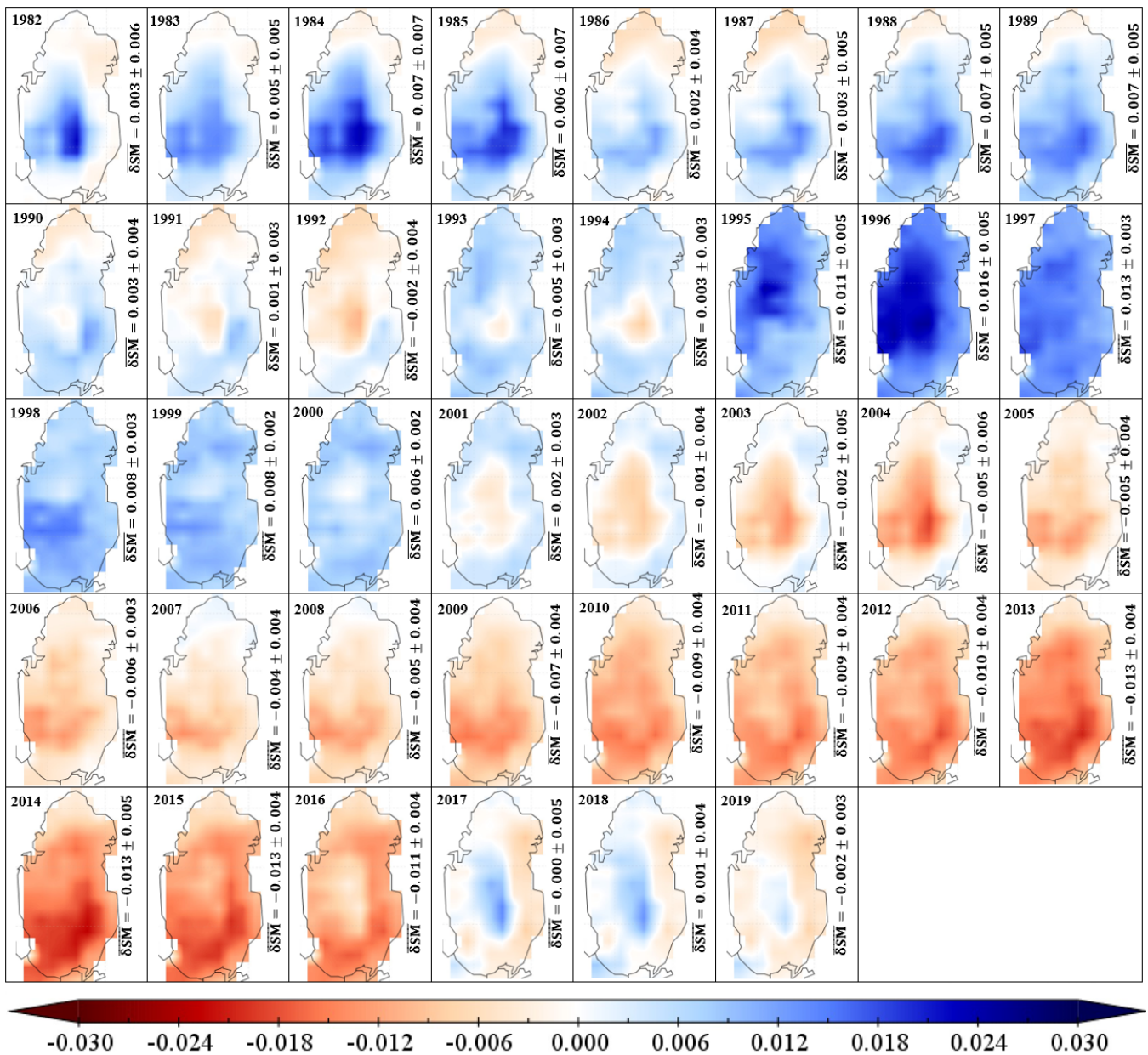


Figure 6. Annual maps of soil moisture anomaly (m^3/m^3) from 1982 to 2019. Spatially-averaged soil moisture anomaly plus/minus one standard deviation is shown on each map.

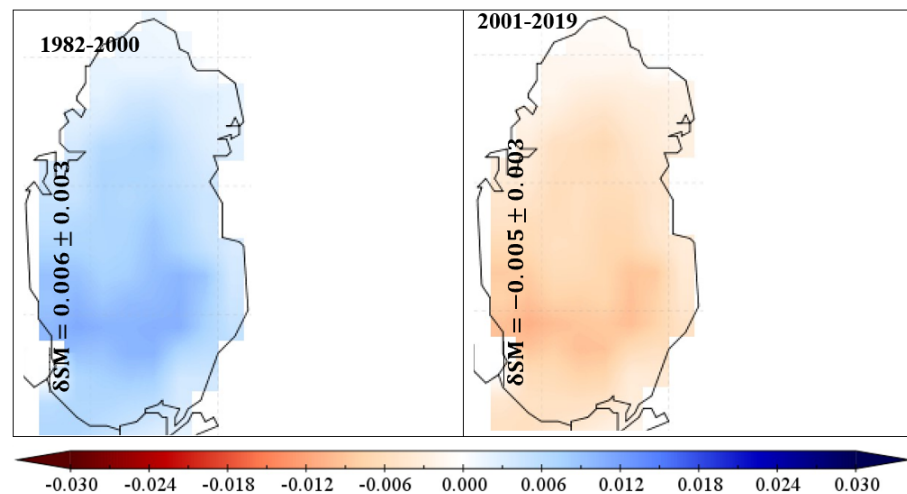


Figure 7. Maps of mean soil moisture anomaly (m^3/m^3) during 1982–2000 (left) and 2001–2019 (right). Spatially-averaged soil moisture anomaly plus/minus one standard deviation is also shown on each map.

Figure 8 shows the maps of annual RF anomalies (δRF) from 1982 to 2019. The largest and lowest anomalies are observed in 1982 and 2010, respectively. Positive rainfall anomalies are seen in 10 years (i.e., 1982, 1983, 1988, 1991–1993, 1995–1997, and 1999) from 1982 to 2000. Negative rainfall anomalies are observed in 11 years (i.e., 2001–2004, 2008, 2010–2014, and 2018) from 2001 to 2019. Also, as shown in Figure 9, the spatially averaged δRF ($\overline{\delta RF}$) indicates a positive (negative) value of 0.25 (−0.20) during 1982–2000 (2001–2019).

In general, both SM and RF declined in 2001–2019 compared to 1982–2000 (Figures 3 and 5). In addition, SM and RF anomalies showed positive values during 1982–2000 and negative values between 2001 and 2019 (Figures 7 and 9). Occurrence of drier years (i.e., negative RF anomaly, Figure 9) with a lower amount of RF (Figure 8) may impact the variations of SM (Figure 6) and its anomaly (Figure 7) in the recent 19 years (2001–2019). However, other factors such as more extraction of groundwater as a result of the growth of population and land use/cover change also affect variations of SM and its anomalies [1].

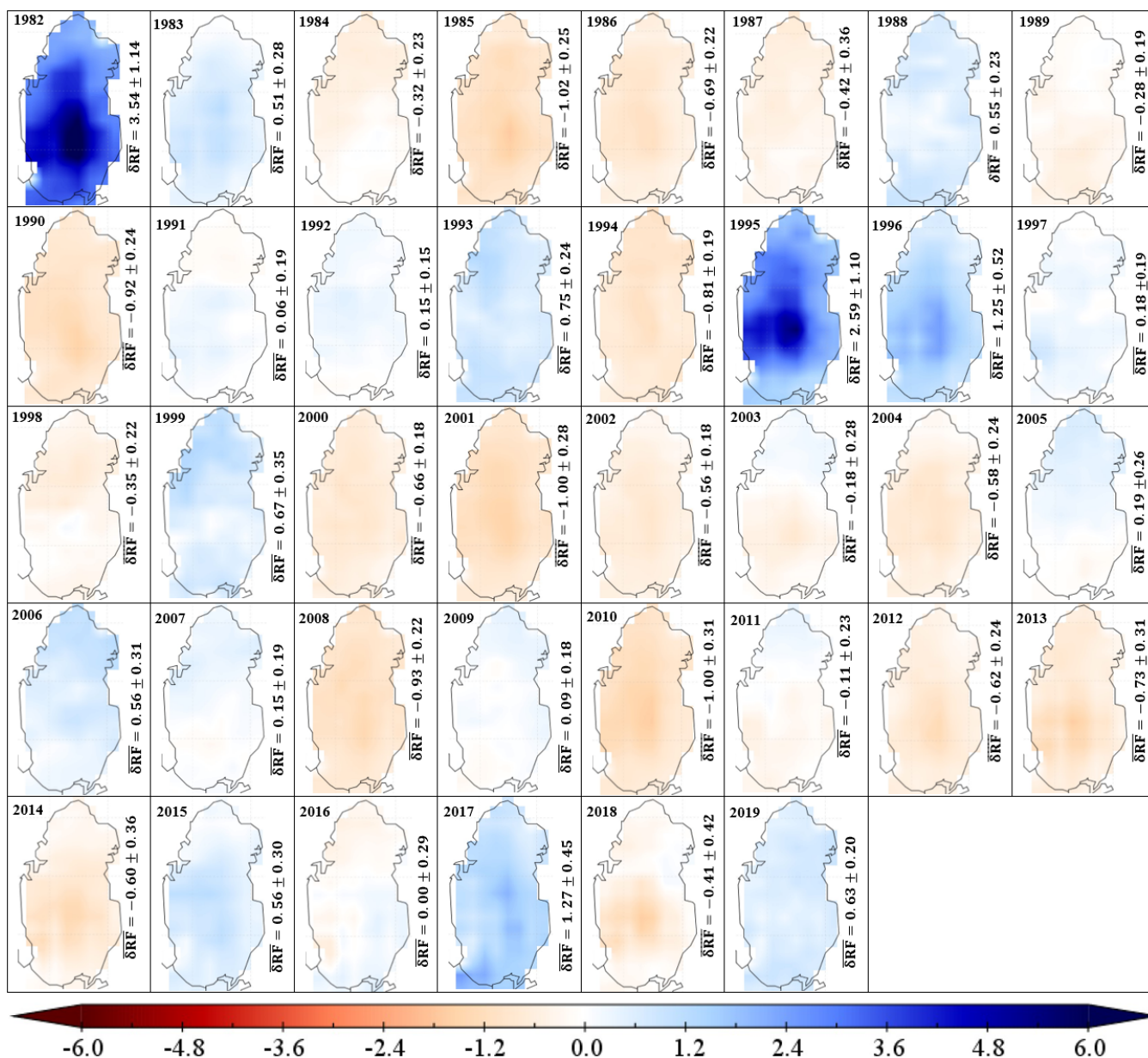


Figure 8. Maps of annual rainfall flux anomaly ($mg/m^2/s$) in Qatar from 1982 to 2019. Spatially-averaged rainfall flux anomaly plus/minus one standard deviation is shown on each map.

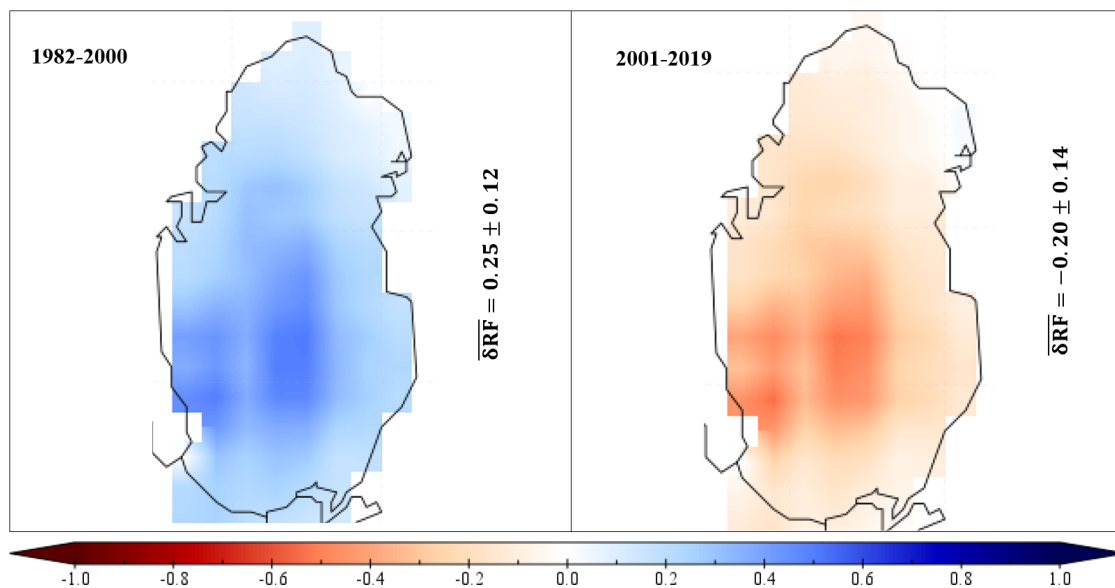


Figure 9. Maps of mean rainfall flux anomaly ($\text{mg}/\text{m}^2/\text{s}$) during 1982–2000 (left) and 2001–2019 (right). Spatially-averaged rainfall flux anomaly plus/minus one standard deviation is also shown on each map.

Figure 10 compares the anomalies of annual rainfall flux and SM at two points in Qatar from 1982 to 2019. The first point is centered at the latitude of 25.05° and longitude of 51.25° (first row), and the second one is located at the latitude of 25.15° and longitude of 51.25° . These two points are chosen because they had the highest amount of annual rainfall flux and soil moisture, and thus have a larger anomaly. As can be seen, the anomalies of annual rainfall flux and SM show consistent fluctuations at both points, implying that SM is mainly controlled by rainfall in Qatar.

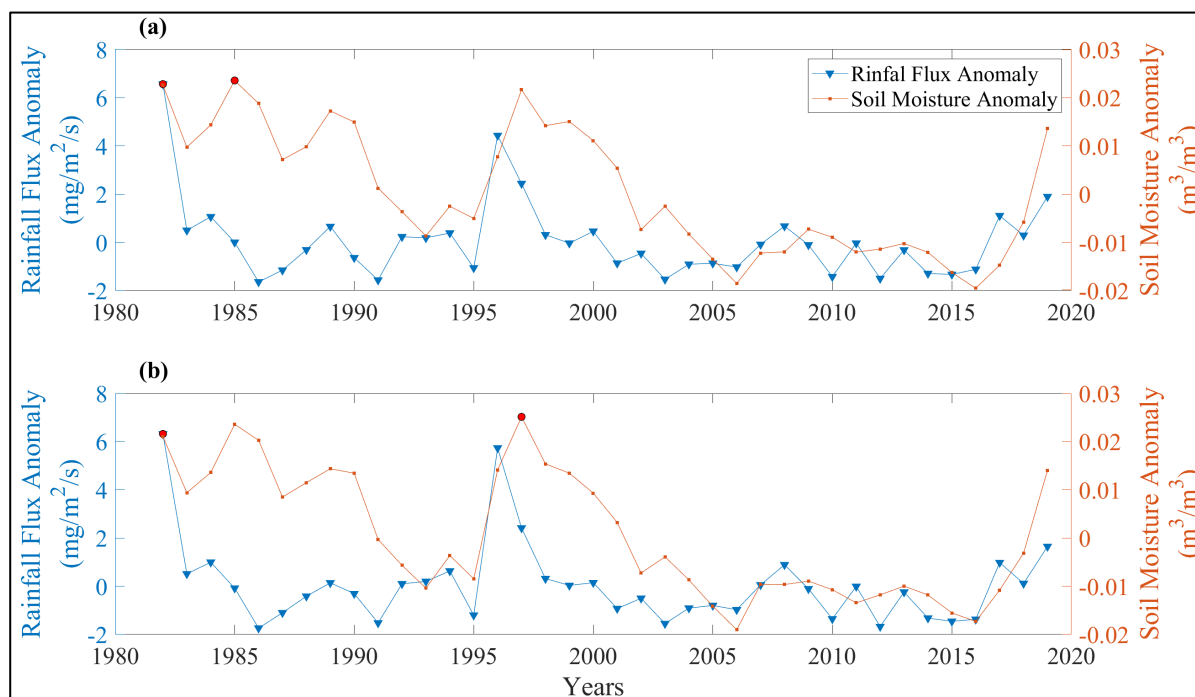


Figure 10. Time series of rainfall flux anomaly (left axis) and soil moisture anomaly (right axis) for the two pixels with the highest amounts of annual rainfall flux and soil moisture. (a) point #1 (latitude: 25.05° and longitude: 51.25°) and (b) point #2 (latitude: 25.15° and longitude: 51.25°). The red circles represent peak years during 1982–2019.

Figure 11 shows annual maps of groundwater storage (GWS) from the Gravity Recovery and Climate Experiment (GRACE) in Qatar from 2003 to 2019. As indicated, GWS in 2012–2019 is less than that of 2003–2011. Also, the lowest amount of GWS can be seen in the northwest and southeast of Qatar. Higher amounts are observed around the center of Qatar. A relatively similar

pattern is observed in SM (Figure 2) and RF (Figure 3) maps that have higher values at the center. Unfortunately, the GRACE GWS data with the resolution of $0.125^\circ \times 0.125^\circ$ is not available in Qatar and thus we had to plot GRACE GWS maps with a lower resolution of $0.25^\circ \times 0.25^\circ$. This difference in spatial resolution over such a small study domain makes the comparison of GRACE GWS and FLDAS SM/RF data difficult.

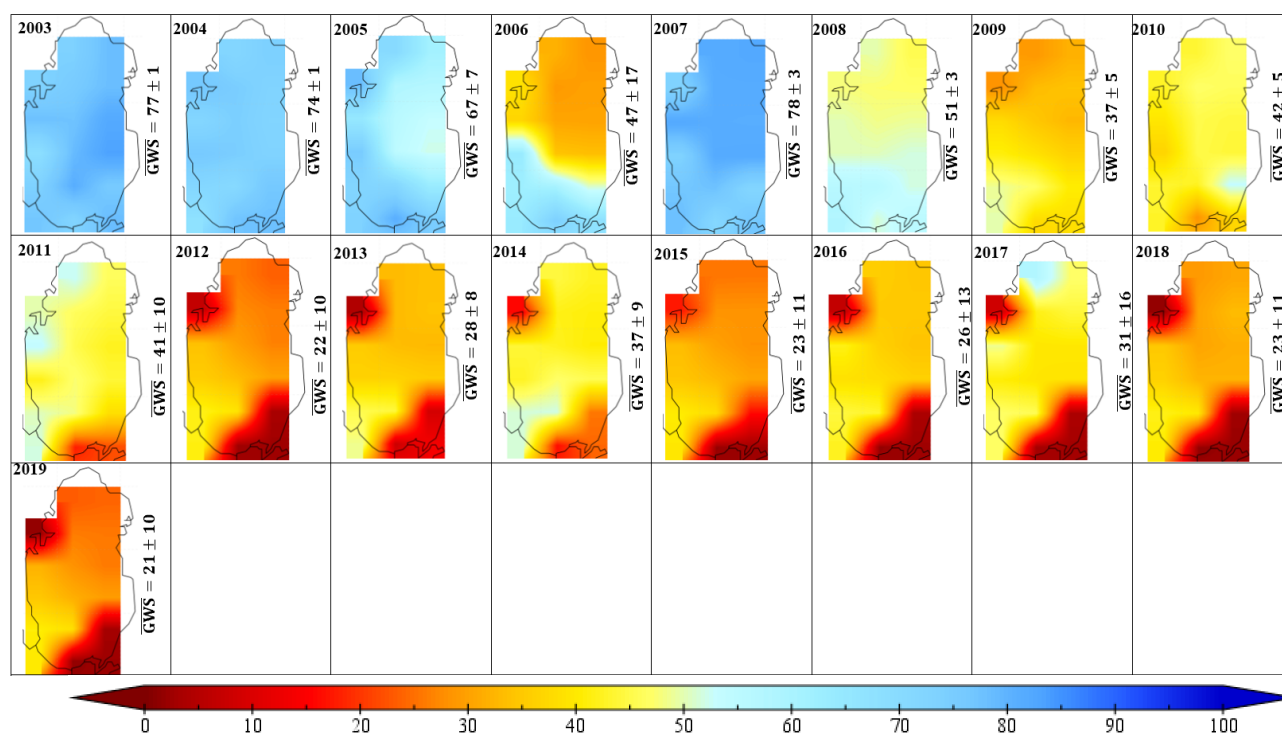


Figure 11. Annual maps of groundwater storage (%) from the Gravity Recovery and Climate Experiment (GRACE) in Qatar from 2003 to 2019. Spatially-averaged groundwater storage (GWS) plus/minus one standard deviation is shown on each map.

Figure 12 shows the locations of sites (blue symbols) in Qatar with the highest mean SM during 1982–2019. These locations have been identified based on the information presented in the Appendix A. The sites are close to Mukaynis and Wadi Jallal. The green/gray circles in the northeast of Mukaynis and southwest of Wadi Jallal represent center-pivot irrigation systems. These irrigation systems are close to the sites with the highest SM. Mukaynis is known as Dark Cave [35]. Ellis [50] found evidence of heavy rainfalls and floods in this area. Wadi Jallal is a village in the Al Wakrah municipality of Qatar, with a potential for the occurrence of floods during heavy rainfalls [51]. According to Grichting [52], Wadi Jallal suffers from flooding and experiences a significant amount of water infiltration. This is in agreement with our results regarding the high values of SM in Wadi Jallal. Therefore, the results of this study may help find the hotspots with the highest SM where there is a higher chance of extracting groundwater resources.

It is worth mentioning that the two sites with the highest SM are located in the area where the water table is at the depth of 1–2 m below the ground (Figure 1) and the hydraulic conductivity is equal to $4 \text{ m}^2/\text{day}$ [34]. Moreover, these two sites have the lowest risk of salinization ($\text{EC} = 3\text{--}4 \text{ mmohs/cm}$) in Qatar [34]. Boron, Lithium, and Molybdenum groundwater concentrations for the selected sites are 1–500, 51–150, and 0–10 ppb, respectively [53]. Moreover, the groundwater vulnerability maps show that these sites are located in an area with very low vulnerability to net recharge, aquifer media, soil media, topography, and hydraulic conductivity [34,53].

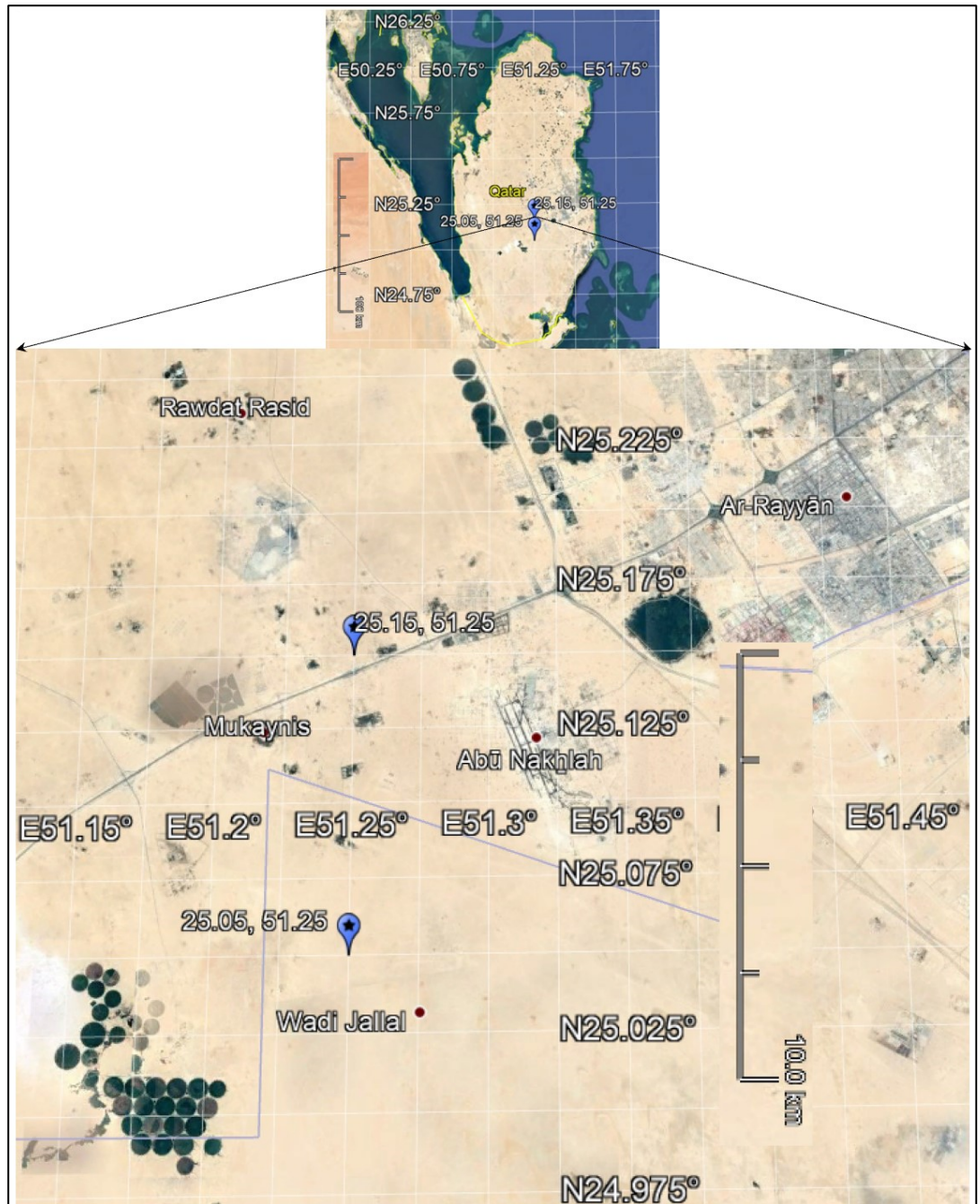


Figure 12. Location of the pixels with the highest soil moisture in the depth 1–2 m in Qatar from 1982 to 2019. White lines represent latitudes and longitudes.

4. Conclusions

This study evaluates the annual variations of soil moisture (SM) (as an indicator of groundwater) and rainfall flux (RF) data in Qatar from 1982 to 2019. The SM at the depth of 1–2 m and RF data are downloaded from the Famine Early Warning Systems Network (FEWS NET) Land Data Assimilation System (FLDAS) available on the National Aeronautics and Space Administration (NASA) archive (<https://earthdata.nasa.gov/>). In general, both SM and RF increased in 1982–2000 and decreased in 2001–2019. SM and RF anomalies were positive during 1982–2000 and negative from 2001 to 2019. Drier years (with the negative RF anomaly) reduced SM in the recent 19 years (2001–2019). Three major rainfall events before 1983, during 1995–1996, and in 2017 recharged groundwater resources and increased SM in the periods 1982–1991, 1995–2000, and 2017–2019, respectively.

The highest SM values in Qatar are observed at two sites near Mukaynis and Wadi Jallal. The center-pivot irrigation systems around these sites indicate their high potential to access

groundwater resources. These sites are also located in the area with the lowest risk of salinization and groundwater vulnerability. The results of this study may help find the hotspots with the highest SM where there is a higher likelihood of groundwater resources. This is helpful for detecting and monitoring groundwater resources in arid environments [54–58]. The output of this research will help water resources engineers understand the sustainability of groundwater resources in Qatar over a long period of about 40 years (1982–2019) because of rainfall events, population increase, and excessive groundwater withdrawal. Moreover, the results can be applied in other similar regions with arid climate. Future studies should be directed towards using remote sensing and/or in-situ SM measurements to assess the accuracy of FLDAS SM data. Also, given the population growth and increasing demands for water resources, analyzing the relationship between human activities and spatiotemporal variations of SM and groundwater resources should be considered for future studies.

Data Availability

The data that support the findings of this study are available from the corresponding author upon reasonable request.

Author Contributions

Conceptualization, M.V.; methodology, M.V.; software, M.V., H.K; validation, M.V., H.K; formal analysis, M.V., H.K.; investigation, M.V., H.K., S.M.B.; resources, M.V., S.M.B.; data curation, M.V., S.M.B; supervision, S.M.B.; writing—original draft preparation, M.V.; writing—review and editing, M.V., H.K, S.M.B., E.H.; All authors have read and agreed to the published version of the manuscript.

Conflicts of Interest

The authors declare no conflict of interest.

References

- Awadh, S.M.; Al-Mimar, H.; Yaseen, Z.M. Groundwater availability and water demand sustainability over the upper mega aquifers of Arabian Peninsula and west region of Iraq. *Environ. Dev. Sustain.* **2021**, *23*, 1–21. <https://doi.org/10.1007/s10668-019-00578-z>
- Schulz, S. Experimental and numerical studies on the water balance of the Upper Mega Aquifer system, Arabian Peninsula. Ph.D. Thesis, Technische Universität Darmstadt, Darmstadt, Germany, 24 March 2017.
- Pike, J.G. Groundwater resources development and the environment in the central region of the Arabian Gulf. *Int. J. Water Resour. Dev.* **1983**, *1*, 115–132. <https://doi.org/10.1080/07900628308722280>
- Baalousha, H.M.; Ouda, O.K.M. Domestic water demand challenges in Qatar. *Arab. J. Geosci.* **2017**, *10*, 537. <https://doi.org/10.1007/s12517-017-3330-4>
- Al-Ibrahim, A.A. Excessive Use of Groundwater Resources in Saudi Arabia: Impacts and Policy Options. *Ambio* **1991**, *20*, 34–37.
- Bakiewicz, W.; Milne, D.M.; Noori, M. Hydrogeology of the Umm Er Radhuma aquifer, Saudi Arabia, with reference to fossil gradients. *Q. J. Eng. Geol. Hydrogeol.* **1982**, *15*, 105–126. <https://doi.org/10.1144/GSL.QJEG.1982.015.02.03>
- Beaumont, P. Water and development in Saudi Arabia. *Geogr. J.* **1977**, *143*, 42–60. <https://doi.org/10.2307/1796674>
- Dirks, H.; Al Ajmi, H.; Kienast, P.; Rausch, R. Hydrogeology of the Umm Er Radhuma Aquifer (Arabian peninsula). *Grundwasser* **2018**, *23*, 5–15. <https://doi.org/10.1007/s00767-017-0388-6>
- Al-Fatlawi, A.N. Hydrogeological study for Umm Er Radhuma Aquifer—West of Iraq. Ph.D. Thesis, Baghdad University, Baghdad, Iraq, 2010.
- Al-Fatlawi, A.N. Geological and hydrogeological characteristics of Umm Er Radhuma aquifer West of Iraq. *Euphrates J. Agric. Sci.* **2010**, *2*, 12–20.
- Koohafkan, A.P. Desertification, drought and their consequences. Environmental and Natural Resources Service Sustainable Development Department, Food and Agriculture Organization (FAO): Rome, Italy, 1996.
- Raghavendra, N.S.; Dekka, P.C. Sustainable development and management of groundwater resources in mining affected areas: A review. *Procedia Earth Planet. Sci.* **2015**, *11*, 598–604. <https://doi.org/10.1016/j.proeps.2015.06.061>
- Sayl, K.N.; Muhammad, N.S.; Yaseen, Z.M.; El-shafie, A. Estimation the Physical Variables of Rainwater Harvesting System Using Integrated GIS-Based Remote Sensing Approach. *Water Resour. Manag.* **2016**, *30*, 3299–3313. <https://doi.org/10.1007/s11269-016-1350-6>
- Almazroui, M.; Saeed, F.; Saeed, S.; Islam, M.N.; Ismail, M.; Klutse, N.A.B.; Siddiqui, M.H. Projected Change in Temperature and Precipitation Over Africa from CMIP6. *Earth Syst. Environ.* **2020**, *4*, 455–475. <https://doi.org/10.1007/s41748-020-00161-x>
- Ghorbani, M.A.; Deo, R.C.; Yaseen, Z.M.; Kashani, M.H.; Mohammadi, B. Pan evaporation prediction using a hybrid multilayer perceptron-firefly algorithm (MLP-FFA) model: case study in North Iran. *Theor. Appl. Climatol.* **2018**, *133*, 1119–1131. <https://doi.org/10.1007/s00704-017-2244-0>

16. Qutbudin, I.; Shiru, M.S.; Sharafati, A.; Ahmed, K.; Al-Ansari, N.; Yaseen, Z.M.; Shahid, S.; Wang, X. Seasonal Drought Pattern Changes Due to Climate Variability: Case Study in Afghanistan. *Water* **2019**, *11*, 1096. <https://doi.org/10.3390/w11051096>
17. Salih, S.Q.; Allawi, M.F.; Yousif, A.A.; Armanuos, A.M.; Saggi, M.K.; Ali, M.; Shahid, S.; Al-Ansari, N.; Yaseen, Z.M.; Chau, K.-W. Viability of the advanced adaptive neuro-fuzzy inference system model on reservoir evaporation process simulation: Case study of Nasser Lake in Egypt. *Eng. Appl. Comput. Fluid Mech.* **2019**, *13*, 878–891. <https://doi.org/10.1080/19942060.2019.1647879>
18. Odhiambo, G.O. Water scarcity in the Arabian Peninsula and socio-economic implications. *Appl. Water Sci.* **2017**, *7*, 2479–2492. <https://doi.org/10.1007/s13201-016-0440-1>
19. Kalhor, K.; Emaminejad, N. Sustainable development in cities: Studying the relationship between groundwater level and urbanization using remote sensing data. *Groundw. Sustain. Dev.* **2019**, *9*, 100243. <https://doi.org/10.1016/j.gsd.2019.100243>
20. Lanjwani, M.F.; Khuhawar, M.Y.; Jahangir Khuhawar, T.M.; Lanjwani, A.H.; Jagirani, M.S.; Kori, A.H.; Rind, I.K.; Khuhawar, A.H.; Dodo, J.M. Risk assessment of heavy metals and salts for human and irrigation consumption of groundwater in Qambar city: A case study. *Geol. Ecol. Lands.* **2020**, *4*, 23–39. <https://doi.org/10.1080/24749508.2019.1571670>
21. Bedaso, Z.K.; Wu, S.-Y.; Johnson, A.N.; McTighe, C. Assessing groundwater sustainability under changing climate using isotopic tracers and climate modelling, southwest Ohio, USA. *Hydrol. Sci. J.* **2019**, *64*, 798–807. <https://doi.org/10.1080/02626667.2019.1606429>
22. Das, B.; Pal, S.C. Assessment of groundwater recharge and its potential zone identification in groundwater-stressed Goghat-I block of Hugli District, West Bengal India. *Environ. Dev. Sustain.* **2020**, *22*, 5905–5923. <https://doi.org/10.1007/s10668-019-00457-7>
23. Niaz, A.; Khan, M.R.; Ijaz, U.; Yasin, M.; Hameed, F. Determination of groundwater potential by using geoelectrical method and petrographic analysis in Rawalakot and adjacent areas of Azad Kashmir, sub-Himalayas, Pakistan. *Arab. J. Geosci.* **2018**, *11*, 468. <https://doi.org/10.1007/s12517-018-3811-0>
24. Pande, C.B.; Moharir, K.N.; Singh, S.K.; Varade, A.M. An integrated approach to delineate the groundwater potential zones in Devdari watershed area of Akola district, Maharashtra, Central India. *Environ. Dev. Sustain.* **2020**, *22*, 4867–4887. <https://doi.org/10.1007/s10668-019-00409-1>
25. Awad, S.R. Groundwater hydrogeology and quality in Helwan area and its vicinities in Egypt. *Water Sci.* **2019**, *33*, 10–21. <https://doi.org/10.1080/11104929.2019.1624307>
26. Ali, M.E.; Abdel-Hameed, M. The potential of nitrate removal from groundwater of Bani-Suif west area, Egypt using nanocomposite reverse osmosis membranes. *J. Bas. Environ. Sci.* **2018**, *5*, 230–239.
27. Chowdhury, S.; Al-Zahrani, M. Characterizing water resources and trends of sector wise water consumptions in Saudi Arabia. *J. King Saud Univ. Eng. Sci.* **2015**, *27*, 68–82. <https://doi.org/10.1016/j.jksues.2013.02.002>
28. Taylor, R.; Scanlon, B.; Döll, P.; Rodell, M.; van Beek, R.; Wada, Y.; Longuevergne, L.; Leblanc, M.; Famiglietti, J.S. Ground water and climate change. *Nature Clim. Change* **2013**, *3*, 322–329. <https://doi.org/10.1038/nclimate1744>
29. Lezzaik, K.; Milewski, A.; Mullen, J. The groundwater risk index: development and application in the Middle East and North Africa region. *Sci. Total Environ.* **2018**, *628*, 1149–1164. <https://doi.org/10.1016/j.scitotenv.2018.02.066>
30. Hussein, H.; Lambert, L.A. A Rentier State under Blockade: Qatar's Water-Energy-Food Predicament from Energy Abundance and Food Insecurity to a Silent Water Crisis. *Water* **2020**, *12*, 1051. <https://doi.org/10.3390/w12041051>
31. Al Hajri, M.M.; Shadid, F.T.; Al-Hajri, K.; Ahmed, S. Qualitative and quantitative assessment of drained water from urban ground-water. *Eng. J. Qatar Univ.* **1992**, *5*, 237–248.
32. Ministry of Development Planning and Statistics (MDPS). Water Statistics in the State of Qatar 2015; Ministry of Development Planning and Statistics: Doha, Qatar, 2017.
33. Ministry of Development Planning and Statistics (MDPS). Water Statistics in the State of Qatar, Doha; Ministry of Development Planning and Statistics: Doha, Qatar, 2018.
34. Baalousha, H.M. Groundwater vulnerability mapping of Qatar aquifers. *J. Afr. Earth Sci.* **2016**, *124*, 75–93. <https://doi.org/10.1016/j.jafrearsci.2016.09.017>
35. Sadiq A.M.; Nasir S.J. Middle Pleistocene karst evolution in the State of Qatar, Arabian Gulf. *J. Cave Karst Stud.* **2002**, *64*, 132–139.
36. Giorgi, F. Climate change hot-spots. *Geophys. Res. Lett.* **2006**, *33*, 1–4. <https://doi.org/10.1029/2006GL025734>
37. Dee, D.P.; Uppala, S.M.; Simmons, A.J.; Berrisford, P.; Poli, P.; Kobayashi, S.; Andrae, U.; Balmaseda, M.A.; Balsamo, G.; Bauer, P.; et al. The ERA-Interim reanalysis: Configuration and performance of the data assimilation system. *Q. J. R. Meteorol. Soc.* **2011**, *137*, 553–597. <https://doi.org/10.1002/qj.828>
38. Solomon, S.; Manning, M.; Marquis, M.; Qin, D. Climate change 2007-the physical science basis: Working group I contribution to the fourth assessment report of the IPCC (Vol. 4). Cambridge University Press: Cambridge, UK, 2007.
39. McNally, A.; Arsenault, K.; Kumar, S.; Shukla, S.; Peterson, P.; Wang, S.; Funk, C.; Peters-Lidard, C.D.; Verdin, J.P. A land data assimilation system for sub-Saharan Africa food and water security applications. *Sci. Data* **2017**, *4*, 170012. <https://doi.org/10.1038/sdata.2017.12>
40. Morris, J.D.; Collopy, J.J. Water use and salt accumulation by *Eucalyptus camaldulensis* and *Casuarina cunninghamiana* on a site with shallow saline groundwater. *Agric. Water Manag.* **1999**, *39*, 205–227. [https://doi.org/10.1016/S0378-3774\(98\)00079-1](https://doi.org/10.1016/S0378-3774(98)00079-1)
41. Harvey, J.W.; Odum, W.E. The influence of tidal marshes on upland groundwater discharge to estuaries. *Biogeochemistry* **1990**, *10*, 217–236. <https://doi.org/10.1007/BF00003145>
42. Vadas, P.A.; Srinivasan, M.S.; Kleinman, P.J.A.; Schmidt, J.P.; Allen, A.L. Hydrology and groundwater nutrient concentrations in a ditch-drained agroecosystem. *J. Soil Water Conserv.* **2007**, *62*, 178–188.
43. Xia, M.; Ma, L.; Shi, Q.; Chen, Z.; Zhou, J. The Relationship of NO₃-N Leaching and Rainfall Types During Summer Fallow in the Loess Plateau Dryland. *Sci. Agric. Sin.* **2018**, *51*, 1537–1546. <https://doi.org/10.3864/j.issn.0578-1752.2018.08.010>
44. Sarkar, T.; Kannaujia, S.; Taloor, A.K.; Ray, P.K.C.; Chauhan, P. Integrated study of GRACE data derived interannual groundwater storage variability over water stressed Indian regions. *Groundw. Sustain. Dev.* **2020**, *10*, 100376. <https://doi.org/10.1016/j.gsd.2020.100376>

45. Diouf, O.C.; Weihermüller, L.; Diedhiou, M.; Vereecken, H.; Faye, S.C.; Faye, S.; Sylla, S.N. Modelling groundwater evapotranspiration in a shallow aquifer in a semi-arid environment. *J. Hydrol.* **2020**, *587*, 124967. <https://doi.org/10.1016/j.jhydrol.2020.124967>
46. Wang, S.; Liu, H.; Yu, Y.; Zhao, W.; Yang, Q.; Liu, J. Evaluation of groundwater sustainability in the arid Hexi Corridor of Northwestern China, using GRACE, GLDAS and measured groundwater data products. *Sci. Total Environ.* **2020**, *705*, 135829. <https://doi.org/10.1016/j.scitotenv.2019.135829>
47. Hameed, M.; Ahmadalipour, A.; Moradkhani, H. Drought and food security in the middle east: An analytical framework. *Agric. For. Meteorol.* **2020**, *281*, 107816. <https://doi.org/10.1016/j.agrformet.2019.107816>
48. Valipour, M.; Bateni, S.M.; Gholami Sefidkouhi, M.A.; Raeini-Sarjaz, M.; Singh, V.P. Complexity of forces driving trend of reference evapotranspiration and signals of climate change. *Atmosphere* **2020**, *11*, 1081. <https://doi.org/10.3390/atmos11101081>
49. Valipour, M.; Sefidkouhi, M.A.G.; Raeini-Sarjaz, M. Selecting the best model to estimate potential evapotranspiration with respect to climate change and magnitudes of extreme events. *Agric. Water Manag.* **2017**, *180*, 50–60. <https://doi.org/10.1016/j.agwat.2016.08.025>
50. Ellis, M. Caves in Qatar. *SMCC J.* **2004**, *13*, 324–331.
51. The Centre for Geographic Information Systems of Qatar. District Map. Retrieved 4 January 2019. https://en.wikipedia.org/wiki/Wadi_Jallal (assessed 22 July 2020).
52. Grichting, A. Blue Design for Urban Resilience in Drylands: The Case of Qatar. In *Nature Driven Urbanism*; Roggema, R., Ed.; Springer: Cham, Switzerland, 2020; pp. 175–208.
53. Ahmad, A.Y.; Al-Ghouti, M.A. Approaches to achieve sustainable use and management of groundwater resources in Qatar: A review. *Groundw. Sustain. Dev.* **2020**, *11*, 100367. <https://doi.org/10.1016/j.gsd.2020.100367>
54. Lee, J.J.; O'Neill, I.J. US-Qatar Partnership Aims to Find Buried Water in Earth's Deserts. Available online: <https://climate.nasa.gov/news/3024/us-qatar-partnership-aims-to-find-buried-water-in-earths-deserts/> (assessed 12 October 2020).
55. Abotalib, A.Z.; Heggy, E.; Scabbia, G.; Mazzoni, A. Groundwater dynamics in fossil fractured carbonate aquifers in Eastern Arabian Peninsula: A preliminary investigation. *J. Hydrol.* **2019**, *571*, 460–470. <https://doi.org/10.1016/j.jhydrol.2019.02.013>
56. Heggy, E. Probing groundwater in arid environments: challenges and opportunities south of the Mediterranean basin. *Euro-Mediterr. J. Environ. Integr.* **2018**, *3*, 42. <https://doi.org/10.1007/s41207-018-0084-7>
57. USDA. Conservation Innovation Grants. Available online: <https://www.nrcs.usda.gov/wps/portal/nrcs/detailfull/national/programs/financial/cig/?cid=stelprdb1045412> (assessed 28 October 2020).
58. Ismail, A.M.A. The quality of irrigation ground-water in Qatar and its effect on the development of agriculture. *J. Arid Environ.* **1984**, *7*, 101–106. [https://doi.org/10.1016/S0140-1963\(18\)31405-8](https://doi.org/10.1016/S0140-1963(18)31405-8)

Appendix A

In this study, we used 110 pixels for the FLDAS SM and RF data over Qatar. Table A1 shows the latitude and longitude associated with each pixel number (PN) in Qatar. The pixel numbers start (PN = 1) with the lowest latitude and longitude in the southwest of Qatar (24.45 °N, 51.05 °E) and continue to the last pixel (PN = 110) with the highest latitude and longitude in the northeast of Qatar (26.15 °N, 51.25 °E).

Table A1. Latitudes and longitudes associated with pixel numbers in Qatar.

Pixel Number	Latitude (°N)	Longitude (°E)	Pixel Number	Latitude (°N)	Longitude (°E)	Pixel Number	Latitude (°N)	Longitude (°E)
1	24.45	51.05	41	25.05	51.25	80	25.55	51.35
2	24.45	51.15	42	25.05	51.35	81	25.55	51.45
3	24.45	51.25	43	25.05	51.45	82	25.65	50.95
4	24.55	50.85	44	25.05	51.55	83	25.65	51.05
5	24.55	50.95	45	25.15	50.85	84	25.65	51.15
6	24.55	51.05	46	25.15	50.95	85	25.65	51.25
7	24.55	51.15	47	25.15	51.05	86	25.65	51.35
8	24.55	51.25	48	25.15	51.15	87	25.65	51.45
9	24.55	51.35	49	25.15	51.25	88	25.65	51.55
10	24.65	50.85	50	25.15	51.35	89	25.75	50.95
11	24.65	50.95	51	25.15	51.45	90	25.75	51.05
12	24.65	51.05	52	25.15	51.55	91	25.75	51.15
13	24.65	51.15	53	25.25	50.85	92	25.75	51.25
14	24.65	51.25	54	25.25	50.95	93	25.75	51.35
15	24.65	51.35	55	25.25	51.05	94	25.75	51.45
17	24.75	50.95	56	25.25	51.15	95	25.75	51.55
18	24.75	51.05	57	25.25	51.25	96	25.85	51.05
19	24.75	51.15	58	25.25	51.35	97	25.85	51.15
20	24.75	51.25	59	25.25	51.45	98	25.85	51.25
21	24.75	51.35	60	25.25	51.55	99	25.85	51.35
22	24.75	51.45	61	25.35	50.85	100	25.85	51.45
23	24.85	50.95	62	25.35	50.95	101	25.85	51.55
24	24.85	51.05	63	25.35	51.05	102	25.95	51.05
25	24.85	51.15	64	25.35	51.15	103	25.95	51.15
26	24.85	51.25	65	25.35	51.25	104	25.95	51.25
27	24.85	51.35	66	25.35	51.35	105	25.95	51.35
28	24.85	51.45	67	25.35	51.45	107	26.05	51.15
29	24.95	50.85	68	25.45	50.85	108	26.05	51.25
30	24.95	50.95	69	25.45	50.95	109	26.05	51.35
31	24.95	51.05	70	25.45	51.05	110	26.15	51.25
32	24.95	51.15	71	25.45	51.15			
33	24.95	51.25	72	25.45	51.25			
34	24.95	51.35	73	25.45	51.35			
35	24.95	51.45	74	25.45	51.45			
36	24.95	51.55	75	25.55	50.85			
37	25.05	50.85	76	25.55	50.95			
38	25.05	50.95	77	25.55	51.05			
39	25.05	51.05	78	25.55	51.15			
40	25.05	51.15	79	25.55	51.25			

Figure A1a–d indicates the mean variation of SM and RF in each pixel over 1982–2019 (a 38-year period), 2010–2019 (the recent 10 years), 2017–2019 (the recent 3 years), and 2019, respectively. A horizontal black line is plotted to easily identify all pixels with $SM \geq 0.350 \text{ m}^3/\text{m}^3$. As can be seen, in each figure, the same pixels have the highest SM and RF values, which clarifies the dominant impact of RF on SM (Figures 2–9). In Figure A1, two pixels (PN = 49 and PN = 41) have the highest SM. PN = 49 has a latitude of 25.15 °N and a longitude of 51.25 °E. PN = 41 has a latitude of 25.05 °N and a longitude of 51.25 °E.

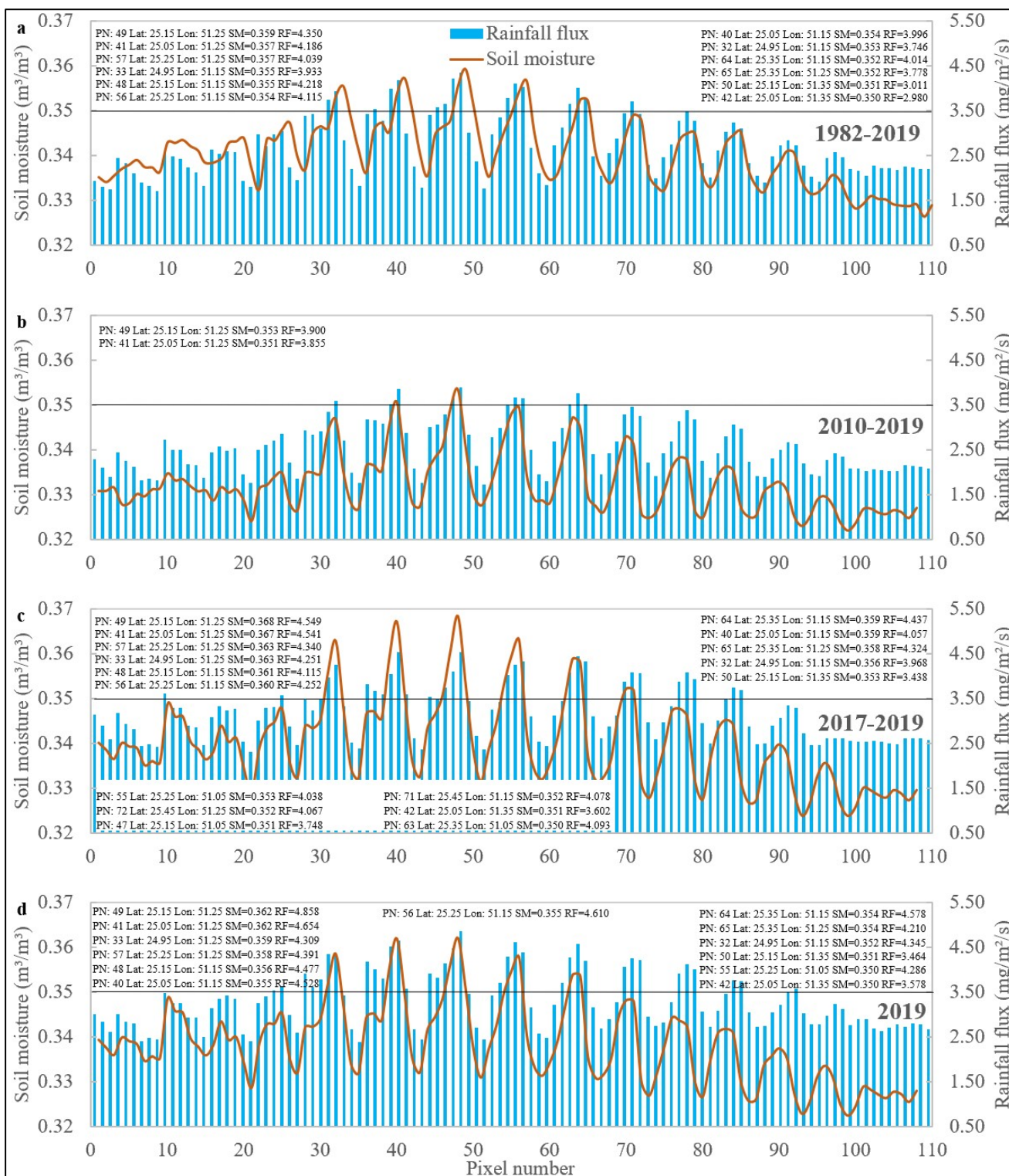


Figure A1. Mean variations of soil moisture (m^3/m^3) and rainfall flux ($\text{mg}/\text{m}^2/\text{s}$) in each pixel over (a) 1982–2019 (a 38-year period), (b) 2010–2019 (the recent 10 years), (c) 2017–2019 (the recent 3 years), and (d) 2019. PN, Lat, Lon, SM, and RF represent pixel number, latitude, longitude, soil moisture, and rainfall flux, respectively.